

Universality in Surface Mixing Rule of Adsorption Strength for Small Adsorbates on Binary Transition Metal Alloys

Jeonghyun Ko¹, Hyunguk Kwon¹, Hyejin Kang¹, Byung-Kook Kim², and Jeong Woo Han^{1,*}

¹*Department of Chemical Engineering, University of Seoul, Seoul 130-743, Korea*

²*High Temperature Energy Materials Center, Korea Institute of Science and Technology,
Seoul 136-791, Korea*

Supplementary Information

S1. Crystal structure information

We obtained the equilibrium lattice parameters via DFT-PBE functional. The DFT-optimized lattice parameters are in good agreement with the experimental results (Table S1).[1]

Metal	Structure	DFT (this work)		Experiment[1]	
		a (Å)	c (Å)	a (Å)	c (Å)
Ni(111)	fcc	3.53	—	3.52	—
Fe(110)	bcc	2.83	—	2.87	—
Cu(111)	fcc	3.64	—	3.61	—
Co(0001)	hcp	2.49	4.02	2.51	4.07
Ir(111)	fcc	3.88	—	3.84	—
Ru(0001)	hcp	2.73	4.30	2.71	4.28
Pt(111)	fcc	3.98	—	3.92	—
Pd(111)	fcc	3.96	—	3.89	—
Rh(111)	fcc	3.84	—	3.80	—
Au(111)	fcc	4.18	—	4.08	—
Ag(111)	fcc	4.16	—	4.09	—

Table S1: Comparison of DFT-calculated lattice parameters to the experimental data.

*Correspondence to jwhan@uos.ac.kr

S2. Adsorption on pure metal surfaces

The adsorption of atomic H is the most stable at the fcc hollow site on pure metal surfaces, except for Fe(110) and Ir(111), with the adsorption energies from -0.74 to -0.05 eV. Our adsorption results are in good agreement with the previous reports.[2–9] Both hollow sites (i.e. hcp and fcc hollow sites) are energetically favored on most of pure metal surfaces. For Fe(110), atomic H prefers to adsorb onto the long bridge site which is highly coordinated in this surface. In general, the adsorbates are adsorbed strongly at high coordination sites because the adsorbate-metal interactions are maximized.[10] Exceptionally, H atom is adsorbed preferentially at the top site of Pt(111) and Ir(111).[4–6]

Atomic O adsorbs on the pure metal surfaces with the adsorption energies from -3.50 to -0.57 eV. Similarly to the atomic H, atomic O also prefers to the hollow sites on pure metal surfaces.[2,8] The hcp hollow site is the most stable adsorption site of the atomic O for Co(0001) and Ru(0001) while 3-fold hollow site is the most stable site for Fe(110). For the other metal surfaces, fcc hollow site is the most favored for O adsorption. The fcc hollow site is preferred for the adsorption of atomic O on Ir(111) and Pt(111), where atomic H is stably adsorb at top site of them.[2,6,11,12]

Atomic S adsorbs on the pure metal surfaces with adsorption energies from -6.19 to -4.16 eV. Similarly to the other species, the adsorption of S is preferred to adsorb at hollow sites.[6,7,13–18] The adsorption of S strongly favors the hcp hollow site for Ru(0001) and Rh(111) and the long bridge site for Fe(110), respectively. On the other hand, the fcc hollow site is favorable on the other metals.

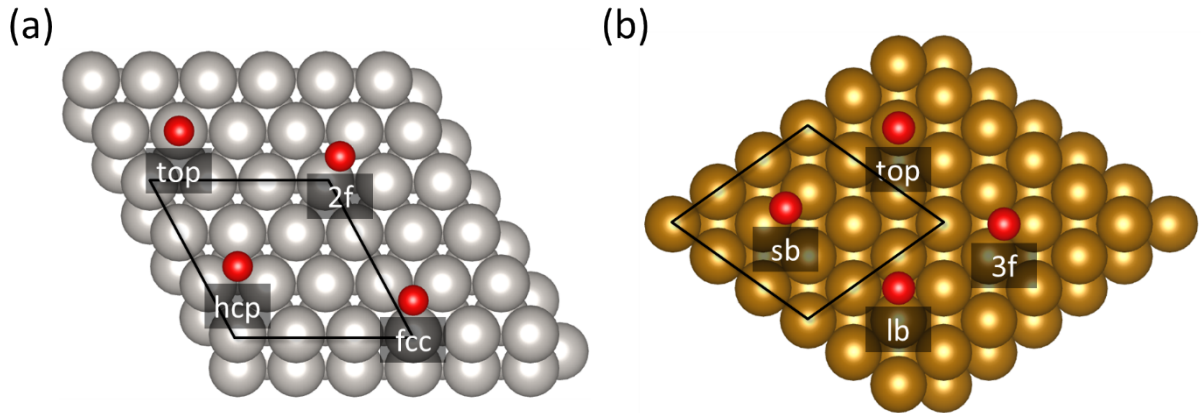


Figure S1: Top view of the adsorption sites on each pure metal surface. (a) hcp(0001) and fcc(111) and (b) bcc(110).

CO molecule is adsorbed on pure metal surfaces with the adsorption energies from -2.30 to -0.59 eV. As shown in Fig. S2(a), CO vertically adsorbs on the metal surfaces with the C atom towards the surface. It also exists that CO molecule is tilted orientated to the metal surfaces,[19] which is indicated in the asterisk (*) in Table S2. For the most of cases, it tends to prefer to adsorb in the hollow sites.[20] For Ir(111), CO molecule stably adsorbs at top site. For Ru(0001), both top and hcp hollow sites are energetically degenerated on the adsorption of CO.[6,21] A bridge site is preferred on Au(111). Largest adsorption energies are observed at hcp hollow sites on Ni(111), Ru(0001) and Rh(111), respectively. The adsorption at fcc hollow site is preferred on Cu(111), Co(0001), Pt(111), Pd(111), and Ag(111). For Fe(110), 3-fold hollow is preferred upon the CO adsorption.[7,22,23]

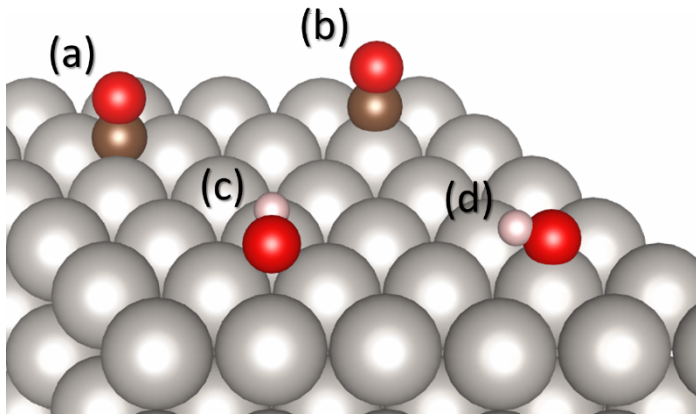


Figure S2: The adsorption structures of CO or OH molecule. CO molecule vertically adsorbs at (a) the hollow and (b) the top sites. OH molecule is tilted upon the adsorption at (c) the 2-fold bridge and (d) the top sites. C, H, and O atoms are denoted by dark brown, light pink and red balls, respectively.

OH molecule is adsorbed on pure metal surfaces with adsorption energies from -4.21 to -2.49 eV. It has been known that the O atom of OH molecule is towards the metal surfaces upon the adsorption.[2] In our DFT calculations, The OH adsorption on hollow and tilted bridge sites are energetically favorable for pure metal surfaces. The hcp hollow site is preferred on Co(0001) and Ru(0001) while the fcc hollow site is preferred on Ni(111), Cu(111), Pd(111), Rh(111), Au(111) and Ag(111). For Fe(110), 3-fold hollow site is most favorable.[2,7] On the other hand, OH molecule is preferentially adsorbed at the 2-fold bridge site on Ir(111) and Pd(111). The adsorption energies of OH are degenerated at the fcc hollow and 2-fold bridge site on Pd(111).[2] It is noteworthy that OH is tilted away from the surface when the adsorption occurs at the top or 2-fold bridge sites on pure metal surfaces (see Fig. S2(c), (d)).[2,6] The tilted top site is preferred for the OH adsorption on Pt(111).

Metal	H		O		S		CO		OH	
	site	E_{ads} (eV)								
Ni(111)	fcc	-0.63	fcc	-2.47	fcc	-5.58	hcp	-2.21	fcc	-3.51
Fe(110)	lb	-0.74	3f	-3.50	lb	-6.13	3f	-2.13	3f	-4.21
Cu(111)	fcc	-0.38	fcc	-1.97	fcc	-5.00	fcc	-1.26	fcc	-3.45

Co(0001)	fcc	-0.60	hcp	-2.72	fcc	-5.54	fcc	-2.02	hcp	-3.46
Ir(111)	top	-0.55	fcc	-1.97	fcc	-5.83	top	-2.27	bridge*	-2.98
Ru(0001)	fcc	-0.73	hcp	-3.03	hcp	-6.19	top	-2.21	hcp	-3.63
							hcp	-2.21		
Pt(111)	top	-0.61	fcc	-1.33	fcc	-5.51	fcc	-2.04	top*	-2.58
	fcc	-0.61								
Pd(111)	fcc	-0.69	fcc	-1.43	fcc	-5.35	fcc	-2.30	bridge*	-2.76
							fcc			-2.76
Rh(111)	fcc	-0.61	fcc	-2.19	hcp	-5.88	hcp	-2.29	fcc	-3.17
Au(111)	fcc	-0.12	fcc	-0.57	fcc	-4.32	bridge	-0.83	fcc	-2.49
Ag(111)	fcc	-0.05	fcc	-0.78	fcc	-4.16	fcc	-0.59	fcc	-2.94

Table S2: The adsorption energies (in eV) of small species (H, O, S, CO and OH) on pure metal surfaces.

S3. Adsorption on binary metal alloy surfaces

According to the arrangement of solute and host atoms on binary alloy surface, it is possible to exist several kinds of surface alloy patterns. It can be largely categorized into ordered and disordered patterns. Here, we assume that surface alloys have the ordered pattern and avoid the island formation of solute atoms. Under the assumptions, we choose 2 patterns (P1 and P2) for fcc and hcp structure and 3 patterns (P3, P4 and P5) for bcc structure (Fig. 1(a)~(e) in the manuscript). To find the surfaces with the most stable alloy patterns, we calculate the total energies of bare alloy surfaces (Table S3).

fcc(111) / hcp(0001)	Pattern		fcc(111) / hcp(0001)	Pattern	
	P1 (eV)	P2 (eV)		P1 (eV)	P2 (eV)
Cu/Ni	-249.66 (0.10)	-249.76 (0.00)	Ag/Ir	-394.47 (0.32)	-394.79 (0.00)
Pt/Ni	-258.20 (0.00)	-257.71 (0.49)	Ni/Ru	-408.16 (0.00)	-407.98 (0.18)
Pd/Ni	-255.03 (0.00)	-254.81 (0.21)	Fe/Ru	-416.13 (0.00)	-415.95 (0.22)
Rh/Ni	-260.89 (0.00)	-260.49 (0.40)	Cu/Ru	-402.58 (0.00)	-402.36 (0.22)
Au/Ni	-249.93 (0.00)	-249.28 (0.65)	Co/Ru	-411.83 (0.00)	-411.66 (0.17)
Ag/Ni	-246.93 (0.00)	-246.56 (0.36)	Ir/Ru	-419.96 (0.00)	-419.91 (0.05)
Pd/Cu	-179.66 (0.00)	-179.24 (0.42)	Pt/Ru	-411.35 (0.06)	-411.42 (0.00)
Au/Cu	-173.96 (0.00)	-173.42 (0.54)	Pd/Ru	-408.09 (0.34)	-408.44 (0.00)
Ag/Cu	-170.86 (0.00)	-170.63 (0.23)	Rh/Ru	-414.52 (0.08)	-414.60 (0.00)
Ni/Co	-319.12 (0.02)	-319.14 (0.00)	Au/Ru	-402.93 (0.00)	-402.90 (0.03)

Cu/Co	-313.03 (0.00)	-312.99 (0.04)	Ag/Ru	-399.90 (0.13)	-400.03 (0.00)
Ir/Co	-329.96 (0.00)	-329.61 (0.34)	Au/Pt	-266.42 (0.24)	-266.66 (0.00)
Pt/Co	-322.09 (0.00)	-321.71 (0.38)	Ag/Pt	-264.63 (0.44)	-265.06 (0.00)
Pd/Co	-318.70 (0.00)	-318.64 (0.05)	Au/Pd	-240.70 (0.00)	-240.60 (0.10)
Rh/Co	-324.69 (0.00)	-324.46 (0.23)	Ag/Pd	-238.56 (0.11)	-238.67 (0.00)
Au/Co	-313.13 (0.00)	-312.57 (0.56)	Ni/Rh	-330.47 (0.00)	-330.24 (0.23)
Ag/Co	-310.04 (0.00)	-309.74 (0.30)	Cu/Rh	-325.27 (0.00)	-325.14 (0.14)
Cu/Ir	-397.02 (0.06)	-397.08 (0.00)	Pt/Rh	-333.35 (0.00)	-333.29 (0.06)
Pt/Ir	-405.49 (0.00)	-405.43 (0.06)	Pd/Rh	-330.61 (0.00)	-330.60 (0.01)
Pd/Ir	-402.98 (0.01)	-402.99 (0.00)	Au/Rh	-325.55 (0.00)	-325.45 (0.10)
Rh/Ir	-409.13 (0.00)	-409.10 (0.03)	Ag/Rh	-322.90 (0.07)	-322.97 (0.00)
Au/Ir	-396.93 (0.23)	-397.16 (0.00)			

bcc(110)	Pattern		
	P3 (eV)	P4 (eV)	P5 (eV)
Ni/Fe	-365.54 (0.31)	-365.52 (0.33)	-365.85 (0.00)
Cu/Fe	-359.57 (0.00)	-358.93 (0.64)	-359.32 (0.25)
Co/Fe	-369.88(0.15)	-370.00 (0.03)	-370.03 (0.00)
Ir/Fe	-375.98 (0.72)	-376.70 (0.00)	-376.70 (0.00)
Ru/Fe	-375.44 (0.21)	-375.56 (0.09)	-375.65 (0.00)
Pt/Fe	-367.92 (1.08)	-368.85 (0.15)	-369.00 (0.00)
Pd/Fe	-365.04 (0.55)	-365.08 (0.51)	-365.59 (0.00)
Rh/Fe	-371.00 (0.73)	-371.57 (0.15)	-371.73 (0.00)
Au/Fe	-358.87 (0.92)	-359.21 (0.58)	-359.79 (0.00)
Ag/Fe	-356.15 (0.56)	-356.00 (0.70)	-356.70 (0.00)

* The values in parenthesis are total energies relative to the most stable surface configuration.

Table S3: The total energies (in eV) of bare surface of fcc(111), hcp(0001) and bcc(110) surfaces as a function of surface patterns.

Table S4 summarizes the site preferences and energetics of adsorption. Unlike Table S2, the configurations of surrounding atoms near the adsorption site are added. For Cu/Rh(111), atomic H adsorbs on the fcc hollow site surrounded by one Cu atom and two Rh atoms with the adsorption energy of -0.53 eV. We define the notation for this case as “Cu-Rh-Rh”, the surrounding atoms written in a clockwise direction (Fig. S3(a)). For Ir/Fe(110), when atomic H adsorbs at the long bridge site as shown in Fig. S3(b), we notate the surrounding atoms as

“Ir-Fe-Fe-Fe” written in a clockwise direction. The examples of these cases are shown in Fig. S3.

Atomic H adsorbs on the alloy surfaces with the adsorption energies of $-0.98 \sim -0.07$ eV. In general, atomic H prefers to adsorb on the hollow site. However, alloys that contain Pt or Ir as host metal generally favor the top site of the host metal atoms upon the adsorption. It means that the characteristics of these pure metals are largely reflected in the adsorption on their alloy surfaces.

Atomic O and S adsorb on the alloy surfaces with the adsorption energies of $-3.36 \sim -0.75$ eV and $-6.49 \sim -4.19$ eV, respectively. In most cases, hollow sites are energetically stable for these adsorptions. There are several alloys in which bridge sites are favored upon the adsorption (see Table S4). Usually, the atomic adsorbates on the alloy surfaces tend to be adsorbed at the hollow sites and prefer to bind near the element that have larger adsorption energy of the adsorbate.

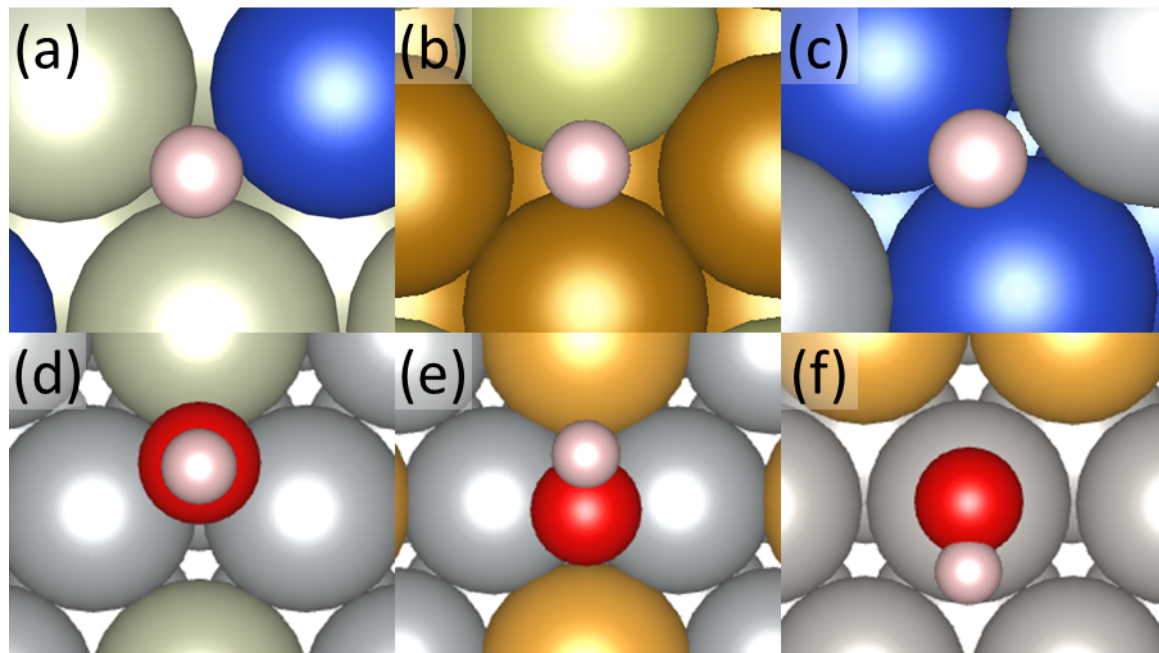


Figure S3: The notation of atomic H and molecular OH adsorption sites that depend on the surrounding atoms. Atomic H is adsorbed on (a) Cu/Rh(111) fcc hollow site: Cu-Rh-Rh, (b) Ir/Fe(110) long bridge site: Ir-Fe-Fe-Fe and (c) Ag/Cu(111) 2-fold bridge site: Cu-Cu. Cu,

Rh, Ni, Ir, Fe, and Ag atoms are denoted by blue, pale green, gray, yellow green, dark gold, and dark gray balls, respectively. Molecular OH is adsorbed on (d) Rh/Ni(111) hcp hollow site: Rh-Ni-Ni, (e) Au/Ni(111) tilted 2-fold bridge site: [Au] Ni-Ni and (f) Au/Pt(111) tilted top site: [Pt-Pt] Pt. Rh, Ni, Au, and Pt atoms are denoted by pale green, gray, gold, and dark gray balls, respectively.

CO adsorbs on the alloy surfaces with the adsorption energies of $-2.55 \sim -0.77$ eV. Similarly to the pure metal surfaces, CO usually prefers to vertically bind on the alloy surfaces except for Cu/Fe(110), Pt/Fe(110), Pd/Fe(110), Au/Fe(110), and Ag/Fe(110). OH adsorbs on alloy surfaces with the adsorption energies of $-4.16 \sim -2.51$ eV. As described earlier, the tilted cases are marked with the asterisk (*) in Table S4. In addition, we use the square brackets to explain the direction of tilting. For instance, Fig. S3(e) shows that OH adsorbs at the 2-fold bridge site between two Ni atoms on Au/Ni(111), which is tilted towards the Au atoms. We denote this case as “[Au] Ni-Ni”. Another example is the adsorption of OH on the top site of Pt atom on Au/Pt(111) in Fig. S3(f). OH is tilted towards the middle between the other two adjacent Pt atoms. This case is denoted as “[Pt-Pt] Pt”.

Surface	Pattern	H			O			S		
		Site ^a	Surrounds ^{b, c}	E _{ads} (eV)	Site ^a	Surrounds ^{b, c}	E _{ads} (eV)	Site ^a	Surrounds ^{b, c}	E _{ads} (eV)
Cu/Ni	P2	fcc	Ni-Ni-Ni	-0.65	fcc	Ni-Ni-Ni	-2.50	fcc	Ni-Ni-Ni	-5.63
Pt/Ni	P1	fcc	Pt-Ni-Ni	-0.41	fcc	Pt-Ni-Ni	-1.55	fcc	Pt-Ni-Ni	-4.93
Pd/Ni	P1	fcc	Pd-Ni-Ni	-0.49	fcc	Pd-Ni-Ni	-1.86	bridge	Ni-Ni	-5.25
Rh/Ni	P1	fcc	Rh-Ni-Ni	-0.53	fcc	Rh-Ni-Ni	-2.07	fcc	Rh-Ni-Ni	-5.33
Au/Ni	P1	fcc	Au-Ni-Ni	-0.28	bridge	Ni-Ni	-1.20	bridge	Ni-Ni	-4.60
Ag/Ni	P1	bridge	Ni-Ni	-0.48	bridge	Ni-Ni	-1.83	bridge	Ni-Ni	-4.99
Ni/Fe	P5	3-fold	Fe-Fe-Fe	-0.65	3-fold	Fe-Fe-Fe	-3.30	long bridge	Fe-Ni-Fe-Fe	-5.88
Cu/Fe	P3	long bridge	Fe-Fe-Fe-Fe	-0.65	long bridge	Fe-Fe-Fe-Fe	-3.33	long bridge	Fe-Fe-Fe-Fe	-6.01
Co/Fe	P5	3-fold	Fe-Fe-Fe-Co	-0.71	3-fold	Fe-Fe-Fe	-3.36	long bridge	Fe-Fe-Fe-Co	-6.00
Ir/Fe	P4	long bridge	Ir-Fe-Fe-Fe	-0.56	long bridge	Ir-Fe-Fe-Fe	-2.68	long bridge	Ir-Fe-Fe-Fe	-5.63
Ru/Fe	P5	3-fold	Ru-Fe-Fe	-0.68	long bridge	Fe-Ru-Fe-Fe	-3.28	long bridge	Fe-Ru-Fe-Fe	-6.10
Pt/Fe	P5	3-fold	Fe-Fe-Fe	-0.60	3-fold	Fe-Fe-Fe	-2.97	long bridge	Fe-Pt-Fe-Fe	-5.52
Pd/Fe	P5	3-fold	Fe-Fe-Fe	-0.62	3-fold	Fe-Fe-Fe	-3.09	long bridge	Fe-Pd-Fe-Fe	-5.75
Rh/Fe	P5	3-fold	Fe-Fe-Fe	-0.59	3-fold	Fe-Fe-Fe	-3.10	long bridge	Fe-Rh-Fe-Fe	-5.85
Au/Fe	P5	3-fold	Fe-Fe-Fe	-0.51	3-fold	Fe-Fe-Fe	-2.81	3-fold	Fe-Fe-Fe	-5.39
Ag/Fe	P5	3-fold	Fe-Fe-Fe	-0.59	3-fold	Fe-Fe-Fe	-3.05	3-fold	Fe-Fe-Fe	-5.63
Pd/Cu	P1	fcc	Pd-Cu-Cu	-0.18	fcc	Pd-Cu-Cu	-1.23	bridge	Cu-Cu	-4.46
Au/Cu	P1	fcc	Au-Cu-Cu	-0.07	fcc	Au-Cu-Cu	-0.96	bridge	Cu-Cu	-4.19
Ag/Cu	P1	bridge	Cu-Cu	-0.23	bridge	Cu-Cu	-1.60	bridge	Cu-Cu	-4.75
Ni/Co	P2	fcc	Ni-Co-Co / Co-Co-Co	-0.56	hcp	Co-Co-Co	-2.69	fcc	Ni-Co-Co	-5.48
Cu/Co	P1	hcp/fcc	Cu-Co-Co	-0.47	fcc	Cu-Co-Co	-2.42	fcc	Cu-Co-Co	-5.30
Ir/Co	P1	fcc	Ir-Co-Co	-0.53	hcp / fcc	Ir-Co-Co	-2.13	fcc	Ir-Co-Co	-5.30
Pt/Co	P1	fcc	Pt-Co-Co	-0.34	fcc	Pt-Co-Co	-1.66	bridge	Co-Co	-4.88
Pd/Co	P1	fcc	Pd-Co-Co	-0.44	bridge	Co-Co	-2.13	bridge	Co-Co	-5.24
Rh/Co	P1	fcc	Rh-Co-Co	-0.53	fcc	Rh-Co-Co	-2.31	bridge	Co-Co	-5.37
Au/Co	P1	hcp	Au-Co-Co	-0.23	bridge	Co-Co	-1.58	bridge	Co-Co	-4.77
Ag/Co	P1	bridge	Co-Co	-0.49	bridge	Co-Co	-2.26	bridge	Co-Co	-5.20
Cu/Ir	P2	fcc	Cu-Ir-Ir	-0.66	fcc	Cu-Ir-Ir	-2.23	fcc	Ir-Ir-Ir	-5.88

Pt/Ir	P1	fcc	Pt-Ir-Ir	-0.43	fcc	Pt-Ir-Ir	-1.59	fcc	Pt-Ir-Ir	-5.51
Pd/Ir	P2	top	Ir	-0.58	fcc	Pd-Ir-Ir	-2.02	fcc	Ir-Ir-Ir	-5.78
Rh/Ir	P1	fcc	Rh-Ir-Ir	-0.56	fcc	Rh-Ir-Ir	-2.04	fcc	Rh-Ir-Ir	-5.85
Au/Ir	P2	top	Ir	-0.57	fcc	Ir-Ir-Ir	-1.79	fcc	Ir-Ir-Ir	-5.70
Ag/Ir	P2	top	Ir	-0.62	fcc	Ir-Ir-Ir	-1.86	fcc	Ir-Ir-Ir	-5.76
Ni/Ru	P1	hcp	Ni-Ru-Ru	-0.68	hcp	Ni-Ru-Ru	-2.87	hcp	Ni-Ru-Ru	-6.11
Fe/Ru	P1	hcp	Fe-Ru-Ru	-0.33	hcp	Fe-Ru-Ru	-3.12	hcp	Fe-Ru-Ru	-6.09
Cu/Ru	P1	hcp	Cu-Ru-Ru	-0.58	hcp	Cu-Ru-Ru	-2.42	hcp	Cu-Ru-Ru	-5.58
Co/Ru	P1	fcc	Co-Ru-Ru	-0.98	hcp	Co-Ru-Ru	-3.34	hcp	Co-Ru-Ru	-6.49
Ir/Ru	P1	hcp	Ir-Ru-Ru	-0.53	hcp	Ir-Ru-Ru	-2.46	hcp	Ir-Ru-Ru	-5.86
Pt/Ru	P2	fcc	Ru-Ru-Ru	-0.62	hcp	Ru-Ru-Ru	-2.53	hcp	Ru-Ru-Ru	-5.89
Pd/Ru	P2	fcc	Ru-Ru-Ru	-0.64	fcc	Ru-Ru-Ru	-2.62	hcp	Ru-Ru-Ru	-5.98
Rh/Ru	P2	fcc	Ru-Ru-Ru	-0.64	hcp	Ru-Ru-Ru	-2.73	hcp	Rh-Ru-Ru	-5.98
Au/Ru	P1	hcp	Au-Ru-Ru	-0.38	hcp	Au-Ru-Ru	-1.62	hcp	Au-Ru-Ru	-5.00
Ag/Ru	P2	fcc	Ru-Ru-Ru	-0.64	fcc	Ru-Ru-Ru	-2.66	fcc	Ru-Ru-Ru	-6.01
Au/Pt	P2	top	Pt	-0.54	fcc	Pt-Pt-Pt	-1.29	fcc	Pt-Pt-Pt	-5.46
Ag/Pt	P2	top	Pt	-0.57	fcc	Pt-Pt-Pt	-1.40	fcc	Pt-Pt-Pt	-5.53
Au/Pd	P1	fcc	Au-Pd-Pd	-0.45	fcc	Au-Pd-Pd	-0.75	fcc	Au-Pd-Pd	-4.61
Ag/Pd	P2	fcc	Pd-Pd-Pd	-0.65	fcc	Pd-Pd-Pd	-1.45	fcc	Pd-Pd-Pd	-5.29
Ni/Rh	P1	fcc	Ni-Rh-Rh	-0.63	fcc	Ni-Rh-Rh	-2.29	fcc	Ni-Rh-Rh	-5.79
Cu/Rh	P1	fcc	Cu-Rh-Rh	-0.53	fcc	Cu-Rh-Rh	-1.94	fcc	Cu-Rh-Rh	-5.36
Pt/Rh	P1	fcc	Pt-Rh-Rh	-0.52	fcc	Pt-Rh-Rh	-1.73	fcc	Pt-Rh-Rh	-5.51
Pd/Rh	P1	fcc	Pd-Rh-Rh	-0.55	fcc	Pd-Rh-Rh	-1.82	fcc	Pd-Rh-Rh	-5.52
Au/Rh	P1	fcc	Au-Rh-Rh	-0.32	fcc	Au-Rh-Rh	-1.13	fcc	Au-Rh-Rh	-4.77
Ag/Rh	P2	fcc	Rh-Rh-Rh	-0.56	fcc	Rh-Rh-Rh	-2.00	fcc	Rh-Rh-Rh	-5.72

Surface	Pattern	CO		OH			
		Site ^a	Surrounds ^{b, c}	E _{ads} (eV)	Site ^a	Surrounds ^{b, c}	E _{ads} (eV)
Cu/Ni	P2	hcp	Ni-Ni-Ni	-2.26	fcc	Ni-Ni-Ni	-3.51
Pt/Ni	P1	hcp	Pt-Ni-Ni	-1.78	bridge*	[Pt] Ni-Ni	-2.70

Pd/Ni	P1	bridge	Ni-Ni	-1.97	bridge*	[Pd] Ni-Ni	-3.05
Rh/Ni	P1	hcp	Rh-Ni-Ni	-2.04	hcp	Rh-Ni-Ni	-3.01
Au/Ni	P1	bridge	Ni-Ni	-1.56	bridge*	[Au] Ni-Ni	-2.65
Ag/Ni	P1	bridge	Ni-Ni	-1.72	bridge*	[Ag] Ni-Ni	-2.98
Ni/Fe	P5	long bridge	Fe-Ni-Fe-Fe	-1.92	3-fold	Fe-Fe-Fe	-4.10
Cu/Fe	P3	3-fold* / long bridge	[Fe] Fe-Fe-Fe / Fe-Fe-Fe-Fe	-2.05	long bridge	Fe-Fe-Fe-Fe	-4.06
Co/Fe	P5	long bridge	Co-Fe-Co-Fe	-2.08	3-fold	Fe-Fe-Fe	-4.16
Ir/Fe	P4	top	Ir	-2.19	short bridge*	[Ir] Fe-Fe	-3.56
Ru/Fe	P5	top	Ru	-2.26	long bridge	Fe-Ru-Fe-Fe	-3.91
Pt/Fe	P5	3-fold*	[Fe] Fe-Fe-Fe	-1.84	3-fold*	[Fe] Fe-Fe-Fe	-3.82
Pd/Fe	P5	top*	[Fe-Fe] Fe	-1.95	3-fold*	[Fe] Fe-Fe-Fe	-3.90
Rh/Fe	P5	top	Rh	-1.95	3-fold	Fe-Fe-Fe	-3.88
Au/Fe	P5	3-fold*	[Fe] Fe-Fe-Fe	-1.86	3-fold*	[Fe] Fe-Fe-Fe	-3.66
Ag/Fe	P5	3-fold*	[Fe] Fe-Fe-Fe	-1.97	3-fold*	[Fe] Fe-Fe-Fe	-3.81
Pd/Cu	P1	fcc	Pd-Cu-Cu	-1.13	fcc	Pd-Cu-Cu	-2.97
Au/Cu	P1	fcc	Au-Cu-Cu	-0.77	bridge*	[Au] Cu-Cu	-2.72
Ag/Cu	P1	bridge	Cu-Cu	-0.96	bridge*	[Ag] Cu-Cu	-3.02
Ni/Co	P2	hcp / fcc	Ni-Co-Co / Co-Co-Co	-1.96	hcp	Co-Co-Co	-3.63
Cu/Co	P1	bridge	Co-Co	-1.84	fcc	Cu-Co-Co	-3.47
Ir/Co	P1	hcp	Ir-Co-Co	-1.93	fcc	Ir-Co-Co	-2.94
Pt/Co	P1	hcp	Pt-Co-Co	-1.54	fcc	Pt-Co-Co	-2.80
Pd/Co	P1	bridge	Co-Co	-1.81	bridge	Ir-Ir	-3.22
Rh/Co	P1	hcp / fcc	Rh-Co-Co	-1.95	fcc	Rh-Co-Co	-3.24
Au/Co	P1	bridge	Co-Co	-1.42	bridge*	[Au] Co-Co	-2.78
Ag/Co	P1	bridge	Co-Co	-1.68	bridge	Co-Co	-3.26
Cu/Ir	P2	top	Ir	-2.45	fcc	Cu-Cu-Ir	-3.24
Pt/Ir	P1	hcp	Pt-Ir-Ir	-1.86	bridge*	[Pt] Ir-Ir	-2.88
Pd/Ir	P2	top	Ir	-2.34	bridge*	[Ir] Ir-Ir	-3.11
Rh/Ir	P1	bridge	Ir-Ir	-2.10	bridge*	[Rh] Ir-Ir	-3.14

Au/Ir	P2	top	Ir	-2.26	bridge*	[Au] Ir-Ir	-3.01
Ag/Ir	P2	top	Ir	-2.34	bridge*	[Ir] Ir-Ir	-3.10
Ni/Ru	P1	hcp	Ni-Ru-Ru	-2.25	hcp	Ni-Ru-Ru	-3.59
Fe/Ru	P1	hcp	Fe-Ru-Ru	-2.11	hcp	Fe-Ru-Ru	-3.48
Cu/Ru	P1	top	Ru	-2.20	hcp	Cu-Ru-Ru	-3.36
Co/Ru	P1	hcp	Co-Ru-Ru	-2.55	hcp	Co-Ru-Ru	-3.95
Ir/Ru	P1	hcp	Ir-Ru-Ru	-2.02	hcp	Ir-Ru-Ru	-3.16
Pt/Ru	P2	top	Ru	-2.04	fcc	Ru-Ru-Ru	-3.57
Pd/Ru	P2	top	Ru	-2.14	fcc	Ru-Ru-Ru	-3.63
Rh/Ru	P2	top	Ru	-2.14	fcc	Ru-Ru-Ru	-3.58
Au/Ru	P1	top	Ru	-1.99	bridge*	[Au] Ru-Ru	-3.00
Ag/Ru	P2	top	Ru	-2.16	fcc	Ru-Ru-Ru	-3.63
Au/Pt	P2	fcc	Pt-Pt-Pt	-1.97	top*	[Pt-Pt] Pt	-2.57
Ag/Pt	P2	bridge	Pt-Pt	-2.04	bridge*	[Pt] Pt-Pt	-2.64
Au/Pd	P1	fcc	Au-Pd-Pd	-1.80	bridge*	[Au] Pd-Pd	-2.51
Ag/Pd	P2	fcc	Pd-Pd-Pd	-2.25	bridge*/fcc	[Pd] Pd-Pd / Pd-Pd-Pd	-2.79
Ni/Rh	P1	fcc	Ni-Rh-Rh	-2.21	fcc	Ni-Rh-Rh	-3.31
Cu/Rh	P1	fcc	Cu-Rh-Rh	-2.07	fcc	Cu-Rh-Rh	-3.13
Pt/Rh	P1	fcc	Pt-Rh-Rh	-2.02	fcc	Pt-Rh-Rh	-2.75
Pd/Rh	P1	fcc	Pd-Rh-Rh	-2.12	bridge*	[Pd] Rh-Rh	-3.10
Au/Rh	P1	bridge	Rh-Rh	-1.76	bridge*	[Au] Rh-Rh	-2.79
Ag/Rh	P2	hcp	Rh-Rh-Rh	-2.19	bridge*	[Rh] Rh-Rh	-3.18

^a top: on top site / bridge: 2-fold bridge site / hcp: hcp hollow site / fcc: fcc hollow site /3-fold: 3-fold hollow site / lb: long bridge site and asterisk (*) indicate that the molecule is tilted from the vertical.

^b The atoms which are surrounding the adsorbate.

^c The label in square brackets indicates the tilted direction of the molecule. (see S3 for the detail).

Table S4: The adsorption energies (in eV) of small molecule (H, O, S, CO and OH) on binary metal surface alloys.

S4. Coverage dependence test of surface mixing rule: The adsorption energies of small adsorbates on Rh/Ir(111) and Ir/Ru(0001) with various solute coverages

Alloy	Coverage (ML)	Pattern ^{a, b}	Total energy (eV)	Pattern ^{a, b}	Total energy (eV)
Rh/Ir(111)	0 (pure Ir(111))	—	-413.93 ^a		
	1/3	P1	-409.13 (0.00)	P2	-409.10 (0.03)
	2/3	rP1	-404.27 (0.00)	rP2	-404.26 (0.01)
	1	—	-399.41 ^a		
Ir/Ru(0001)	0 (pure Ru(0001))	—	-419.36 ^a		
	1/3	P1	-419.96 (0.00)	P2	-419.91 (0.05)
	2/3	rP1	-420.16 (0.00)	rP2	-420.10 (0.06)
	1	—	-419.94 ^a		

* 1/3 ML alloy surface has P1 and P2 patterns while 2/3 ML alloy surface has rP1 and rP2 patterns.

** The values in parenthesis are total energy relative to most stable surface configuration.

^a For 0 and 1 ML alloy surfaces, it is not exist various surface patterns.

^b rP1 and rP2 patterns of upper most layer have the reverse arrangement between solute and host atoms of P1 and P2, respectively (e.g., Fig. S4(b): P1, Fig. S4(c): rP1).

Table S5: The total energies (in eV) of bare surfaces of Rh/Ir(111) and Ir/Ru(0001) with various coverages and surface patterns.

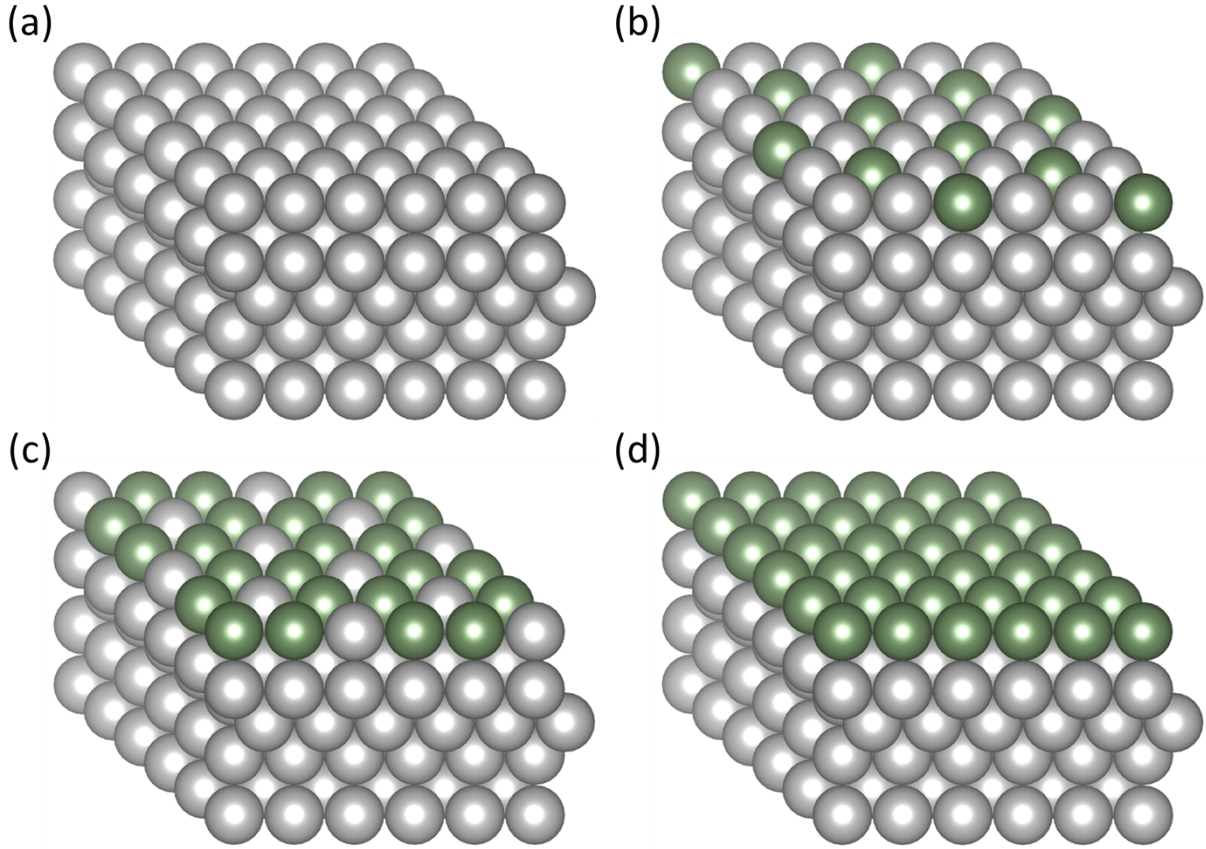


Figure S4: The slab model of bimetallic alloy surface with different solute coverages; (a) 0 ML (same as pure host metal surface), (b) 1/3 ML, (c) 2/3 ML, (d) 1 ML. The solute and host atoms are denoted by the green and gray balls, respectively.

Alloy	Coverage (ML)	H E _{mix} (eV)	H E _{DFT} (eV)	O E _{mix} (eV)	O E _{DFT} (eV)	S E _{mix} (eV)	S E _{DFT} (eV)	CO E _{mix} (eV)	CO E _{DFT} (eV)	OH E _{mix} (eV)	OH E _{DFT} (eV)
Rh/Ir (111)	0	-0.55	-0.55	-1.97	-1.97	-5.83	-5.83	-2.27	-2.27	-2.98	-2.98
	1/3	-0.57	-0.56	-2.04	-2.04	-5.84	-5.85	-2.27	-2.10	-3.04	-3.14
	2/3	-0.59	-0.62	-2.12	-2.11	-5.86	-5.87	-2.28	-2.21	-3.11	-3.15
	1	-0.61	-0.64	-2.19	-2.15	-5.88	-5.87	-2.29	-2.27	-3.17	-3.28
Ir/Ru (0001)	0	-0.73	-0.73	-3.03	-3.03	-6.19	-6.19	-2.21	-2.21	-3.63	-3.63
	1/3	-0.67	-0.53	-2.68	-2.46	-6.07	-5.86	-2.23	-2.02	-3.41	-3.16
	2/3	-0.61	-0.49	-2.33	-2.00	-5.95	-5.61	-2.25	-2.13	-3.19	-3.06
	1	-0.55	-0.49	-1.97	-1.74	-5.83	-5.58	-2.27	-2.10	-2.98	-2.96

Table S6: The comparison between the predicted and the DFT-calculated adsorption energies (in eV) of small adsorbates on Rh/Ir(111) and Ir/Ru(0001) with various solute coverages (0, 1/3, 2/3 and 1 ML). E_{mix} and E_{DFT} are denoted by adsorption energies from the surface mixing rule and the DFT calculation, respectively.

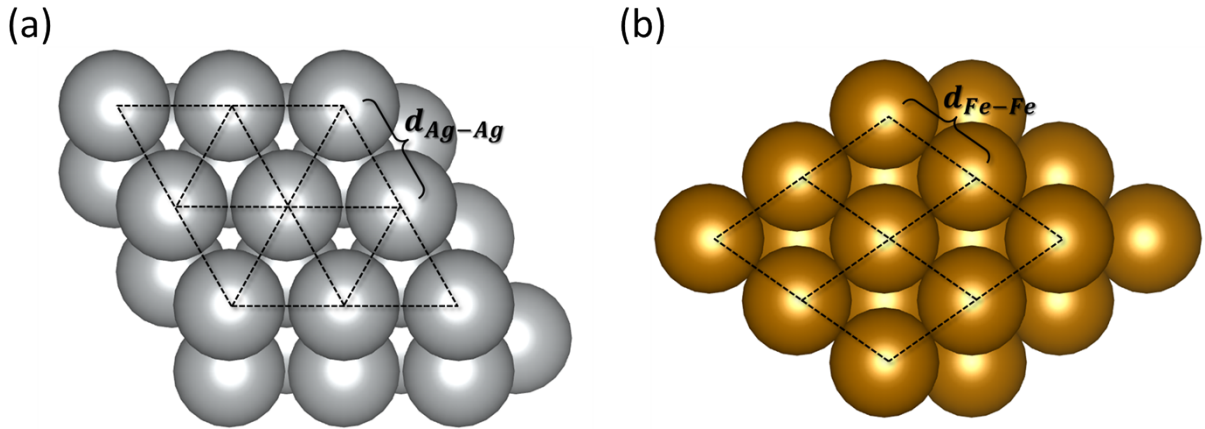


Figure S5: The definition of nearest-neighbor distance (d_{M-M}) of (a) Ag(111) and (b) Fe(110), where M is the transition metal elements. Note that definition of Figure S5(a) represents the fcc(111) and the hcp(0001) while definition of Figure S5(b) represents the bcc(110). For example, *the absolute ratio of nearest-neighbor distance of Ag/Fe(110)* is $d_{Ag/Fe(110)} = d_{Ag(111)-Ag(111)} / d_{Fe(110)-Fe(110)}$.

S5. Application of surface mixing rule: CO oxidation

The corrected adsorption energies are summarized in Table S5 and those are in good agreement with the original adsorption energies from Falsig *et al.*'s.[24] (Fig. S5).

(eV)	This work (PBE)		Falsig[24] (RPBE)		(Falsig) – (ours)		Corrected E _{ads} ^a	
	E _{ads} (O)	E _{ads} (CO)	E _{ads} (O)	E _{ads} (CO)	E _{ads} (O)	E _{ads} (CO)	E _{ads} (O)	E _{ads} (CO)
Ni(111)	-2.47	-2.21	-2.42	-1.29	0.06	0.92	-2.28	-1.35
Fe(110)	-3.50	-2.13	—	—	—	—	-3.30	-1.27
Cu(111)	-1.97	-1.26	-1.67	-0.34	0.31	0.92	-1.78	-0.40
Co(0001)	-2.72	-2.02	—	—	—	—	-2.53	-1.17
Ir(111)	-1.97	-2.27	—	—	—	—	-1.77	-1.41
Ru(0001)	-3.03	-2.21	-2.48	-1.62	0.56	0.59	-2.84	-1.35
Pt(111)	-1.33	-2.04	-1.25	-1.22	0.08	0.82	-1.14	-1.18
Pd(111)	-1.43	-2.30	-1.30	-0.98	0.14	1.32	-1.24	-1.44
Rh(111)	-2.19	-2.29	-2.22	-1.58	-0.03	0.71	-1.99	-1.43
Au(111)	-0.57	-0.83	-0.19	0.12	0.38	0.95	-0.37	0.02
Ag(111)	-0.78	-0.59	-0.69	0.07	0.09	0.65	-0.59	0.27
Average difference (A.D)				0.20	0.86			

^a Corrected adsorption energies are estimated from “(average of the difference) + (ours)”.

Table S7: The adsorption energies (in eV) obtained from our calculations and Falsig *et al.*'s[24] and the corrected adsorption energies.

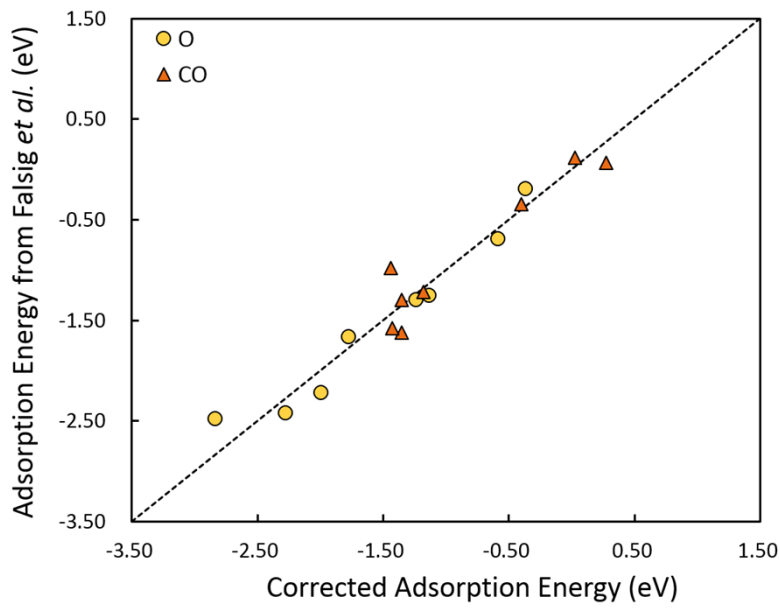


Figure S6: Comparison of the corrected adsorption energies with Falsig *et al.*'s.[24]

Metal	E_{ads} of O (eV)	E_{ads} of CO (eV)	Activity	Price (dollar/kg)
Pt/Ir(111)	-1.60	-1.34	-0.92	35494.97
Pd/Ir(111)	-1.62	-1.27	-0.92	33501.59
Ir(111)	-1.77	-1.41	-0.99	34401.83
Au/Rh(111)	-1.54	-1.01	-1.02	42653.98
Pd(111)	-1.30	-0.98	-1.04	20898.31
Ag/Ir(111)	-1.41	-0.92	-1.05	32172.67
Pt/Rh(111)	-1.90	-1.46	-1.05	42396.77
Rh/Ir(111)	-1.92	-1.47	-1.07	34894.81
Pd/Rh(111)	-1.91	-1.38	-1.08	40403.39
Au/Ru(0001)	-1.72	-1.04	-1.09	7094.71
Ag/Rh(111)	-1.71	-1.03	-1.10	39074.47
Cu/Ir(111)	-1.74	-1.05	-1.10	32108.91
Au/Ir(111)	-1.25	-0.90	-1.11	35752.18
Pt(111)	-1.25	-1.22	-1.15	50798.96
Pt/Ru(0001)	-2.07	-1.49	-1.18	6837.50
Au/Ni(111)	-1.67	-0.82	-1.21	3660.23
Ag/Ru(0001)	-1.88	-1.06	-1.24	3515.20
Pd/Ru(0001)	-2.08	-1.41	-1.25	4844.12
Pt/Ni(111)	-2.03	-1.27	-1.27	3403.02
Rh(111)	-2.22	-1.58	-1.29	41796.61
Ag/Pd(111)	-1.10	-0.63	-1.32	19569.39
Au/Co(0001)	-1.75	-0.74	-1.33	3671.58

Ir/Ru(0001)	-2.24	-1.55	-1.34	5744.35
Pd/Cu(111)	-1.54	-0.56	-1.34	1400.83
Pd/Ni(111)	-2.04	-1.19	-1.35	1409.65
Cu/Rh(111)	-2.03	-1.17	-1.35	39010.71
Ag/Ni(111)	-1.84	-0.84	-1.35	80.73
Ag/Pt(111)	-1.06	-0.79	-1.36	47476.66
Pt/Co(0001)	-2.10	-1.18	-1.42	3414.37
Ni/Rh(111)	-2.28	-1.48	-1.43	39011.34
Au/Cu(111)	-1.17	-0.19	-1.47	3651.42
Rh/Ru(0001)	-2.39	-1.61	-1.47	6237.34
Ag/Co(0001)	-1.91	-0.75	-1.49	92.08
Pd/Co(0001)	-2.12	-1.10	-1.49	1421.00
Ag/Cu(111)	-1.34	-0.21	-1.51	71.92
Cu/Ru(0001)	-2.21	-1.20	-1.53	3451.44
Cu(111)	-1.67	-0.34	-1.54	8.16
Au/Pd(111)	-0.93	-0.61	-1.55	23148.89
Ru(0001)	-2.48	-1.62	-1.56	3697.39
Rh/Ni(111)	-2.35	-1.39	-1.57	2802.87
Ir/Co(0001)	-2.28	-1.25	-1.58	2321.23
Au/Pt(111)	-0.90	-0.77	-1.59	51056.17
Ni/Ru(0001)	-2.46	-1.51	-1.62	3452.07
Cu/Ni(111)	-2.17	-0.98	-1.64	16.97
Co/Ru(0001)	-2.49	-1.47	-1.69	3452.88
Ni(111)	-2.42	-1.29	-1.72	17.60
Rh/Co(0001)	-2.42	-1.30	-1.72	2814.22
Cu/Co(0001)	-2.24	-0.89	-1.78	28.32
Ni/Co(0001)	-2.49	-1.21	-1.86	28.95
Au/Fe(110)	-2.26	-0.81	-1.87	3643.90
Ag(111)	-0.69	0.07	-1.87	964.54
Co(0001)	-2.53	-1.17	-1.93	29.76
Fe/Ru(0001)	-2.75	-1.50	-1.97	3450.91
Pt/Fe(110)	-2.62	-1.25	-1.99	3386.69
Ag/Fe(110)	-2.43	-0.82	-2.06	64.40
Pd/Fe(110)	-2.63	-1.17	-2.06	1393.31
Ir/Fe(110)	-2.79	-1.31	-2.15	2293.55
Rh/Fe(110)	-2.94	-1.37	-2.29	2786.54
Cu/Fe(110)	-2.76	-0.96	-2.35	0.64
Ru/Fe(110)	-3.03	-1.39	-2.38	246.59
Ni/Fe(110)	-3.01	-1.28	-2.43	1.27
Co/Fe(110)	-3.04	-1.23	-2.50	2.08

Au(111)	-0.19	0.12	-2.57	54657.11
Fe(110)	-3.30	-1.27	-2.79	0.10

Table S8: The adsorption energies (in eV) of O and CO and the activity of CO oxidation predicted from them on various pure metals and binary metal alloys. The price (in dollar/kg) of each pure metal and binary metal alloy is also listed.

References

- [1] M.J. Winter, Univ. Sheff. WebElements Ltd, UK. (n.d.), <http://webelements.com/>.
- [2] A.A. Phatak, W.N. Delgass, F.H. Ribeiro, W.F. Schneider, *J. Phys. Chem. C.* 113 (2009) 7269–7276.
- [3] J. Guo, L. Guan, S. Wang, Q. Zhao, Y. Wang, B. Liu, *Appl. Surf. Sci.* 255 (2008) 3164–3169.
- [4] J. Greeley, M. Mavrikakis, *J. Phys. Chem. B.* 109 (2005) 3460–3471.
- [5] P. Ferrin, S. Kandoi, A.U. Nilekar, M. Mavrikakis, *Surf. Sci.* 606 (2012) 679–689.
- [6] W.P. Krekelberg, J. Greeley, M. Mavrikakis, *J. Phys. Chem. B.* 108 (2003) 987–994.
- [7] M. Mavrikakis, J. Rempel, J. Greeley, L.B. Hansen, J.K. Nørskov, *J. Chem. Phys.* 117 (2002).
- [8] M. Pozzo, G. Carlini, R. Rosei, D. Alfè, *J. Chem. Phys.* 126 (2007) 164706.
- [9] J.-F. Paul, P. Sautet, *Surf. Sci.* 356 (1996) L403–L409.
- [10] Y. Gohda, A. Groß, *J. Electroanal. Chem.* 607 (2007) 47–53.
- [11] Y. Xu, M. Mavrikakis, *J. Phys. Chem. B.* 107 (2003) 9298–9307.
- [12] Y. Xu, M. Mavrikakis, *J. Chem. Phys.* 116 (2002) 10846.
- [13] N.M. Galea, J.M.H. Lo, T. Ziegler, *J. Catal.* 263 (2009) 380–389.
- [14] D.R. Alfonso, A. V Cugini, D.S. Sholl, *Surf. Sci.* 546 (2003) 12–26.
- [15] D.R. Alfonso, *Surf. Sci.* 596 (2005) 229–241.
- [16] M. May, S. Gonzalez, F. Illas, *Surf. Sci.* 602 (2008) 906–913.
- [17] S.H. Ma, X.T. Zu, Z.Y. Jiao, H.Y. Xiao, *Eur. Phys. J. B.* 61 (2008) 319–324.
- [18] J. Lahtinen, P. Kantola, S. Jaatinen, K. Habermehl-Cwirzen, P. Salo, J. Vuorinen, M. Lindroos, K. Pussi, A.P. Seitsonen, *Surf. Sci.* 599 (2005) 113–121.
- [19] J. Greeley, A.A. Gokhale, J. Kreuser, J.A. Dumesic, H. Topsøe, N.-Y. Topsøe, M. Mavrikakis, *J. Catal.* 213 (2003) 63–72.
- [20] P. Liu, J.K. Norskov, *Phys. Chem. Chem. Phys.* 3 (2001) 3814–3818.

- [21] F. Abild-Pedersen, M.P. Andersson, *Surf. Sci.* 601 (2007) 1747–1753.
- [22] S. Sakong, C. Mosch, *Phys. Chem. Chem. Phys.* 9 (2007) 2216–2225.
- [23] J. Sivaramakrishna, *AIP Conf. Proc.* 1276 (2010) 413.
- [24] H. Falsig, B. Hvolbaek, I.S. Kristensen, T. Jiang, T. Bligaard, C.H. Christensen, J.K. Nørskov, *Angew. Chem. Int. Ed. Engl.* 47 (2008) 4835–9.